Review Vol. 12, No. 10 / 1 Oct 2022 / Optical Materials Express 3930
Optical Materials EXPRESS

Advanced photonic and optofluidic devices fabricated in glass via femtosecond laser micromachining [Invited]

SIMONE PIACENTINI,[1] FRANCESCA BRAGHERI,[1] GIACOMO CORRIELLI,[1] REBECA MARTÍNEZ VÁZQUEZ,[1] PETRA PAIÈ,[2] AND ROBERTO OSELLAME[1,*]

[1]*Istituto di Fotonica e Nanotecnologie (IFN) - Consiglio Nazionale delle Ricerche (CNR), Piazza Leonardo da Vinci 32, 20133 Milano, Italy*
[2]*Dipartimento di Fisica - Politecnico di Milano, Piazza Leonardo da Vinci 32, 20133 Milano, Italy*
[*]*roberto.osellame@cnr.it*

Abstract: Thanks to its unique properties, glass plays a fundamental role in science and technology, especially in optics and photonics. For instance, its transparency has been exploited in the last decades for efficiently guiding light in optical fibers for long distances, while its versatility makes it the perfect material in different research fields, ranging from fundamental science to biology and chemistry. On the occasion of the International Year of Glass, we would like to discuss a powerful microfabrication technique for devices in this material: femtosecond laser micromachining (FLM). This technique can process different types of glass, and thanks to the nonlinear nature of the induced modification, it enables the fabrication of complex three-dimensional micro-structures capable of guiding light or transporting fluids. The purpose of this review article is to celebrate the multidisciplinary nature of FLM by discussing, without claim for completeness and after a brief introduction about the process, a selection of its applications in the diverse fields of biology, strong-field physics, and astronomy.

1. Introduction

According to scientists, educators, artists, and glass manufacturers across the globe we are at a special moment in time where the arrival of The Age of Glass can be declared. This is surely due to the countless applications of glass, to its infinite recycling possibility and to its possible carbon-free manufacturing [1], all features nowadays highly desirable. Thanks to its properties, glass is exploited in many different fields ranging from food conservation - glass has been in fact selected as the best material for wine storage - to architecture or to optical systems; the international year of glass coincides in fact with the 670th anniversary of the first depiction of eyeglasses in a painting. Transparency is for sure the peculiar feature that drove the use of glass through the years as an optical material exploited in several applications for the manipulation and transport of light possibly in combination with fluids. In the 20th century the encoding of electrical signals into a light beam, in combination with glass transparency, allowed for transmission over long distances with the invention of optical fibers and integrated optical circuits. This led to widespread use of glass products also in communications and electronic industries. In the last decades, thanks to the rapid advancing of science and technology, innovative methods have been developed to produce and microstructure glasses both for photonic and microfluidic devices. For the fabrication of integrated photonic circuits, two main categories can be highlighted: thin film deposition techniques, either physical or chemical, and processes for local modification of the refractive index of the glass, either in bulk or in thin film format [2]. Moreover, the combination of transparency with chemical inertness to many solvents has made glass the material of choice also for the realization of microfluidic devices for many applications, notwithstanding

#463715 https://doi.org/10.1364/OME.463715
Journal © 2022 Received 11 May 2022; revised 7 Jul 2022; accepted 22 Jul 2022; published 13 Sep 2022

Optical Materials EXPRESS

the higher cost of this material with respect to polymers. Fabrication methods for microchannels can be mainly divided into chemical, mechanical and laser-based processes [3,4]. Most of the techniques previously mentioned for the fabrication of optical and microfluidic devices are borrowed from the fabrication of microelectronic chips, as for example photolithography, and can be considered very mature. Nevertheless, their intrinsic capability to process only bidimensional device layouts is a limitation in applications where complex integrated 3D structures are needed. A flexible approach that allows for the fabrication of both optical waveguides and microchannels is femtosecond laser micromachining (FLM), which can be applied to different materials offering a three-dimensional writing capability [5,6]. The use of ultrashort pulses allows controlling the thermal aspects of light-matter interaction [7] and exploiting nonlinear absorption to achieve permanent structuring in transparent materials [8]. These two aspects make ultrashort pulses extremely attractive for glass processing. This review is therefore dedicated to femtosecond laser micromachining of glass as a rapid prototyping technique for photonic and optofluidic devices used in diverse applications. Many recent reviews already cover the basic concepts of FLM and its use for creating glass devices for very different purposes [9–15], therefore here we would like to focus on a restricted set of applications, which are very recent or in rapid expansion and, in our opinion, very promising for FLM in glass. We thus believe that they deserve a dedicated review paper. These are integrated microscopy, on-chip high-harmonic generation and astrophotonics. Another fast growing field of application of FLM in glass is integrated quantum photonics, which however will not be discussed in this paper as some of the authors have very recently published a dedicated review paper, to which we direct the interested readers [14].

2. Femtosecond laser micromachining in glass

FLM in glass is performed by focusing a train of ultrashort laser pulses in the bulk region of the sample by means of a suitable optical system, i.e. an aspheric lens or a microscope objective. Importantly, the laser wavelength must belong to the glass transparency window, in order to prevent its linear absorption. Thanks to the short pulse duration (typically in the range of 50 fs - 500 fs) and the consequent high optical peak intensities reached at the laser focus, non-linear absorption phenomena such as multiphoton absorption and tunnelling ionization are deterministically triggered [16]. This leads to a permanent and localized modification of the substrate on a scale comparable to the size of the laser focal spot. Three-dimensional machining is then achieved by translating the sample at uniform speed, during the laser irradiation, along the desired geometry. Depending on the amount of energy deposited per unit area in the substrate (i.e. the laser fluence), different kinds of modification can be produced, ranging from a smooth and gentle alteration of the refractive index to more dramatic structural changes, up to micro-explosions and cracks. The actual microscopic mechanism that is responsible for these modifications is a complex interplay of different substrate relaxation phenomena upon the laser light absorption [8], whose weights strongly depend on the specific composition of the glass under processing and the irradiation parameters chosen. The main parameters under control are the laser pulse duration and repetition rate, the numerical aperture of the focusing optics, the scan speed and the laser polarization.

2.1. Waveguides

By operating in a low-fluence regime, it is possible to use FLM for inducing a localized increase of the glass refractive index. Such possibility, originally discovered in 1996 by Davis and co-workers [17], plays a major role in the technological applications of FLM, since it allows to write high quality optical waveguides in glass in a direct and maskless fashion, buried in the substrate volume, and with arbitrary 3D layouts. Optical channel waveguides fabricated in this way present a typical refractive index change Δn between core and cladding in the range of

Optical Materials EXPRESS

10^{-3}-10^{-2} and a cross section of a few tens of μm^2, thus featuring guiding properties very similar to those of standard silica fibers.

Most common glass substrates used for FLM waveguide writing, where best results in terms of losses and light confinement have been demonstrated, are pure fused silica [18,19] and several commercial alumino-borosilicate glasses, e.g. Corning Eagle XG, Schott AF32 and Schott Borofloat [20–23]. Single mode light guidance has been obtained in these kinds of glass for the whole visible and near infrared spectrum, up to the telecom C-band, with optimized propagation losses ranging from 0.1 dB/cm to 1 dB/cm, and negligible bending losses for radii of curvature greater than few tens of mm. The waveguide writing in fused silica is preferably performed adopting a low repetition rate regime, i.e. between 1 kHz and 100 kHz. The main physical mechanism responsible for the refractive index increase in this material upon laser irradiation is a local densification due to a re-arrangement of Si-O bonds in the silica network [24]. The waveguides fabricated in this material typically present a strongly elongated cross section, a moderately high degree of modal birefringence (in the order of 10^{-4}) and an elliptical intensity mode profile [25]. For the waveguide inscription in alumino-borosilicate glasses, instead, higher repetition rates are more favourable (i.e. from 500 kHz to 5 MHz). In this regime, the machining process is strongly influenced by thermal accumulation effects [26]. In this case, the major role in the waveguide core formation is played by thermally-induced ion migration processes occurring during the glass melting phase, which are responsible for a local change in the glass chemical composition [27,28]. Waveguides fabricated in these materials present a round cross section, a more circular guided mode profile and a substantially lower degree of birefringence, mainly given by the mechanical stresses that accumulate in the substrate during the machining [29]. In borosilicate glasses it has also been shown that planar waveguides, i.e. light guiding structures where light confinement occurs only in the vertical dimension, can be fabricated by FLM, by irradiating the sample with a high number of laser scans that partially overlap for covering a large horizontal surface, with mm sized width [30].

FLM waveguide fabrication has been demonstrated also in other kind of multi-component glasses besides alumino-borosilicates. One example is represented by zinc-phosphate glasses [31–34], that, thanks to the relative high concentrations of rare-earth ions in their composition, are very attractive for the development of active devices such as waveguide-based lasers and optical amplifiers. Another important example is the FLM waveguide writing in composite chalcogenide glasses such as GLS and fluoride glasses such as ZBLAN. These two materials are particularly appealing for mid-IR photonic applications, thanks to their high degree of transparency in this spectral range. In the case of GLS, waveguides capable of guiding light up to 10 μm wavelength can be fabricated with the multiscan approach, which allows to define a large core cross-section [35–37]. In the case of ZBLAN, instead, the production of positive refractive index change upon direct laser irradiation has proven to be a challenging task. Thus, waveguides in this material are typically fabricated in the so called “depressed-index” configuration, where multiple laser scans opportunely arranged in a 3D fashion are used for defining the waveguide cladding [38–40].

2.2. Microchannels

Another technologically relevant use of FLM applied to glasses is represented by the fabrication of buried three-dimensional hollow channels, whose typical length range from few tens of μm to several mm, suitable for the development of microfluidic and optofluidic devices. This process, mostly applied to fused silica, consists in a two-step procedure commonly known as FLICE: Femtosecond Laser Irradiation followed by Chemical Etching. In particular, the first step consists in using FLM for defining, via laser irradiation, the desired geometry of the channels. If adopting an adequate energy fluence regime, higher than what is required for the waveguide writing process, the irradiation has the effect of creating self-oriented nanogratings, i.e. periodic alterations of the glass morphology at the nanoscale, localized at the laser focal spot and oriented perpendicularly

Optical Materials EXPRESS

to the laser polarization direction [41]. This kind of modification has the macroscopic effect of enhancing locally the etching rate of the substrate when exposed to a wet etching attack. Thus, after irradiation, the sample is immersed in a proper etchant solution, typically hydrofluoric acid (HF), which selectively removes the irradiated material and creates the microchannel structures. This step is favourably performed in a sonic bath, in order to ensure a continuous acid replacement within the channels during the etching process. The finite ratio between the etching rates of the irradiated and non-irradiated material poses some constraint on the possible geometries that can be achieved with the FLICE technique. In particular, in order to fabricate microchannels with an elevated aspect ratio, i.e. with a cross section of few hundreds of μm^2 and a length of several mm, additional strategies must be implemented for a successful outcome. These include the fabrication of additional side-channels, which allow the acid to penetrate in the main structure from multiple access points distributed along its whole length, and to pre-compensate during the irradiation step possible geometry distortions that may arise due to a non-uniform etchant distribution [42]. It has been shown that potassium hydroxide (KOH) [43,44] and Sodium hydroxide (NaOH) [45] can also be used as etching agent for performing FLICE in fused silica, showing a higher etching selectivity for the irradiated vs non-irradiated glass, though at a lower overall etching rate. Finally, besides fused silica, the FLICE process has been demonstrated successfully also in other kind of glasses, including Borofloat 33 [46], Corning Eagle XG borosilicate glass [47], and Schott Foturan [48] a metal-enriched photosensitive glass.

3. Applications

3.1. Microscopy on chip

Lab on a chip devices consisting of microfluidic channels are a powerful tool for the observation of biological samples. Indeed, they allow to analyse the specimens under different and highly controlled conditions, and they facilitate the automation of the measurements by using the fluid flow to deliver the samples through the detection region. Usually, microfluidic channels are fabricated in PDMS substrates by soft lithography, with the advantage that once the mask is developed many replicas can be easily and rapidly obtained. Nevertheless, the poor optical quality of the substrate, the microchannel deformability, the intrinsic bi-dimensional nature of these devices, as well as solvent incompatibility may constitute a limitation for certain applications, such as the one we discuss in this paragraph. On the other side glass substrates are characterized by high optical quality, making them especially suitable for the observation of biological specimens. Imaging is traditionally achieved by placing microfluidics channels in standard bench-top optical microscopes. An increased level of integration can be achieved by fabricating in the same substrate the optical components necessary for sample inspection. In this regard, FLM is an enabling tool for the fabrication of both optical and fluidic components in glass substrates, allowing the on-chip integration of advanced and high throughput imaging techniques.

Hanada and coworkers developed different prototypes of what they referred to as "nano-aquariums" in photostructurable glass substrates (Foturan) for the observation of aquatic microorganisms using external optical setups. Using these devices, they were able to investigate different phenomena, such as i) the flagellum movement of E. Gracilis, a single-celled alga living in fresh water [49], ii) the high-speed motion of a unicellular protist, Criptomona [50] and iii) the gliding mechanism of Phormidium, a genus of filamentous cyanobacteria [51]. In the microfluidic channels they were able to precisely control the environmental conditions, e.g. by dissolving infinitesimal quantities of chemical substances in the water. In addition, by laser irradiation they proved the capability of further customization of the devices. For instance, they have integrated on-chip a movable glass microneedle for the contact stimulation of single cells of Pleurosira laevis, a typical diatom living in fresh water, allowing the observation of information transmission to adjacent cells. Moreover, by the fabrication of two opposites waveguides that face the microchannel they could locally perform optical absorption measurements for environmental

Optical Materials EXPRESS

analysis. Another example of integrated device for the analysis of aquatic microorganisms has been developed by Schaap et al. [52]. While the gold standard protocol for water monitoring is based on sample collection and ex-situ analysis, the compact glass-based optofluidic chip that they proposed is compatible with in-situ measurements, promising a prompt identification of possible phytoplankton outbreaks. This monolithic device is constituted by a curved waveguide, fiber-pigtailed to the laser source at 1550 nm, which is used to illuminate the specimens flowing through a straight microfluidic channel that is a few centimeters long. The waveguide is terminated 500 μm from the microchannel to guarantee the illumination of the entire height of the channel by exploiting the divergence of light at the waveguide output. The signal is externally collected by a four-quadrant photodetector and the light distribution is subsequently analyzed. Using this approach, the authors have been able to successfully classify different algae populations, benefiting from the pattern recognition feature of the neural network toolbox in MATLAB for signal analysis [53].

In the previous application, the use of an optical waveguide for sample illumination has allowed ease of use and a precise and stable alignment between optical and fluidic components. To increase the imaging capabilities of integrated devices also other optical components should be integrated on chip, such as lenses, mirrors or filters. All these components have been successfully fabricated in glass substrates by FLM. Qiao et al. have reported the integration of a microlens and a microfluidic channel in a fused silica substrate, demonstrating image magnification of beads [54]. The lens, fabricated by FLICE, consists of a hole in the substrate with a hemispherical profile, which focuses the light that impinges at the air-glass interface. Since the surface roughness that characterizes this fabrication process could be detrimental for the optical properties of the lens, they used an OH flame to polish the surface. He et al. have reported the fabrication of tunable hemispherical lenses in a photosensitive glass, in which an annealing process is used to smooth the lens surface [55]. Hu et al. have demonstrated lenses with tunable optical properties, by fabricating these optical components inside a microchannel and by filling it with different refractive index liquids (water, ethanol or sucrose solutions) [56]. Paié et al. have reported a cylindrical lens with a profile optimized to reduce spherical aberrations and with dynamically tunable optical properties [57]. Indeed, by combining in the same microfluidic network a droplet generator module and the microfluidic lens, they have been able to obtain an integrated optofluidic modulator capable of both on-demand on/off switching and periodic modulation of light. Dudutis et al., have fabricated by femtosecond laser ablation, followed by CO2 laser polishing a high quality axicon in a fused silica substrate [58], proving properties comparable to the ones of commercially available items. Zhang et al. have presented a microlens array, fabricated by single pulse laser ablation, followed by chemical etching on a fused silica surface [59]. The authors have successfully fabricated a large array with about two millions of microlenses by optimizing a high speed irradiation process, and used it for liquid sensing applications. Wang et al. have reported the fabrication of a micromirror by exploiting total internal reflection at the interface with an embedded hollow trench in a Foturan substrate [60]. They have further integrated it with other optical components, such as waveguides and lenses. Sala et al. have realized the same component in a fused silica substrate. In this work the authors have investigated the parameter optimization of both the laser irradiation and the thermal annealing processes to reduce the surface roughness of microstructures fabricated by FLICE [61].

Benefiting from the capability of FLM to fabricate both high quality optical components and microfluidic channels in glass substrates, Paié et al. have developed a first microscope on a chip based on light sheet fluorescence microscopy (LSFM) [62], for the automatic investigation of fluorescent cellular spheroids. LSFM is a 3D microscopy technique in which a plane of light allows a non-invasive optical sectioning of the sample. In this device, an integrated cylindrical lens, collects the light from a fiber, previously pigtailed to the substrate, and generates a thin plane of light centered in the sample channel, where the specimens are flowing, as in Fig. 1. The

Optical Materials EXPRESS

emitted fluorescence signal is orthogonally collected by an external microscope objective and focused on a camera. Thus, all the specimens flowing in the channel are automatically imaged, with no need of manual alignment or expert end-users. This compact device can be used as an add-on to any standard fluorescence microscope allowing to upgrade it to a light sheet one. In addition, due to the versatility of the fabrication technique, these microscopes on a chip can be easily adapted to the specimens under investigation. Sala et al., have optimized the device for dual color investigation of single cells, by optimizing the channel cross-section and the light sheet thickness, to guarantee an optical sectioning adequate to the cellular dimensions [63]. Memeo et al., have presented a microscope on a chip tailored for Drosophila embryos imaging, whose dimensions can degrade the image quality, being quite thick and elliptical samples (200 x 500 μm^2). In this case, using micro lenses, waveguides, integrated filters and an innovative 3D microchannel layout, both optical and fluidic optimization has been carried out to implement dual-sided illumination and automatic sample orientation [64].

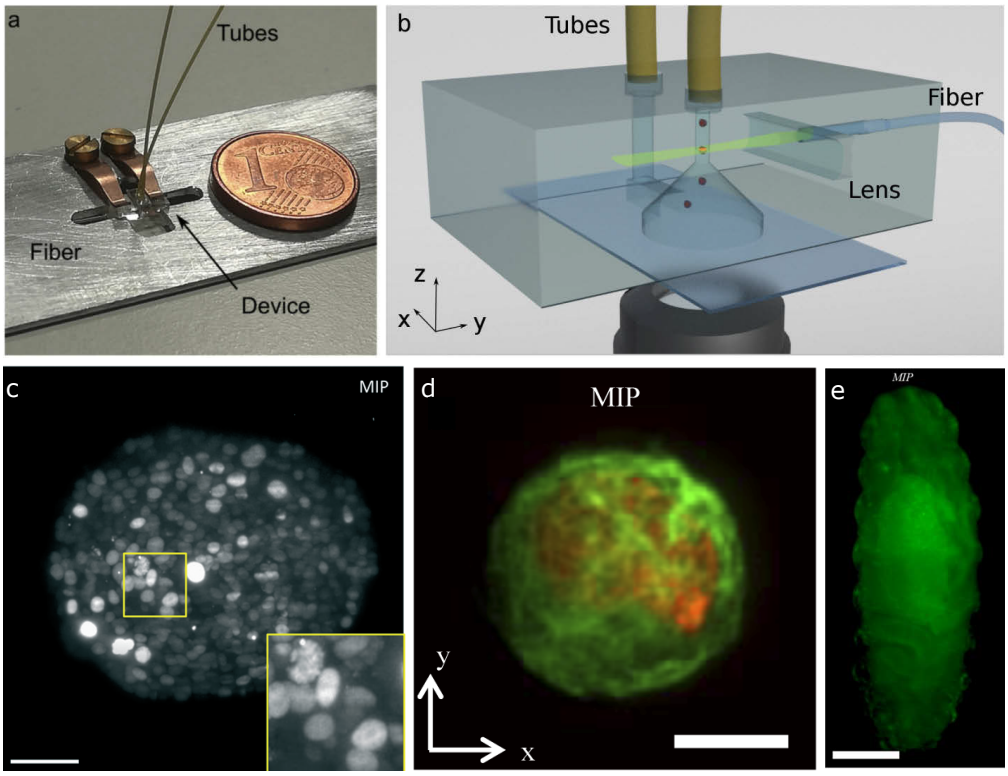

Fig. 1. a) picture and b) schematic design of the microscope on chip for LSFM of single cells. c), d), and e) maximum intensity projections (MIP) of different specimens obtained using stacks of images acquired on chip. Specimens are: a cellular spheroids [62] c), a single cell [61] d), and a Drosophila embryo e) [63], scale bar is 100 µm, 5 µm and 100 µm, respectively.

3.2. *High harmonic generation on chip*

High order Harmonic Generation (HHG) in noble gases is a strongly non-linear process. HHG is driven by the interaction of intense and ultrashort laser pulses with matter; it involves the emission of a burst of coherent radiation, collinear to the driving beam, with a characteristic comb-like spectrum of odd harmonics of the fundamental laser field, ranging from the vacuum ultraviolet to

Optical Materials EXPRESS

the soft x rays [65]. Despite the potentials of this radiation for numerous applications in the field of ultrafast spectroscopy and high-resolution imaging [66,67], coherent light sources of eXtreme ultraviolet (XUV) and soft x-rays based on HHG are confined to a few advanced laboratories and large-scale facilities [68], due to their high technological complexity. Thus HHG in integrated devices paves the way to more compact and easy to align and handle XUV sources. This idea takes origin from the first implementations of HHG in a hollow glass capillary [69]. The capillary is filled with a noble gas and in the meantime it works as a hollow waveguide where the driving field propagates, as a consequence HHG takes place in the capillary core. Hollow waveguides represent a good alternative to the gas jet configuration because they can provide a confined transverse intensity profile of the fundamental beam and thus a very controlled geometry of the interaction region. Nevertheless, the glass capillary strategy presents strong limits regarding the control of the gas density inside them due to the fact that the gas can only access from the two open ends.

In this framework, microfluidic chips fabricated in fused silica glass by the FLICE technique offer several advantages. On the one hand, they are perfectly suitable for the manipulation of gases as the channels are directly buried in glass, a non porous material, thus enabling the possibility to create a microfluidic network to control the gas density. On the other hand, the 3D capabilities of the FLICE technique allows to integrate in the same device the gas microfluidic network and the hollow waveguides, expanding the potentials of HHG in capillaries previously discussed.

The first attempt to use FLICE to produce channels as hollow optical waveguides was made by He et al. in 2011 [70]. They used fused silica substrates to fabricate embedded channels of 250 μm diameter and 100 mm length. For the fabrication they focused a 800-nm wavelength femtosecond laser beam, at 1kHz repetition rate, with a 20x microscope objective (0.46 NA). After irradiation the sample was etched in a 20 M/L aqueous KOH solution, maintained at 95°C. In order to obtain a uniform radius along such long hollow waveguide, they also inscribed short vertical access channels at a constant interval of 5mm, see Fig. 2(a) that facilitates the access of the etchant to the main channel. The samples are afterwards thermally annealed to smooth the hollow waveguide walls, achieving an average roughness of 52.4 nm, in a 50x50 μm^2 area. Thanks to this high surface smoothness they achieve a transmission of 90% with an He-Ne laser, which is close to the theoretical limit of 95%. They also demonstrated the capability to couple and propagate in the same waveguides a femtosecond laser beam at 800-nm wavelength (Fig. 2(b) and (c)) with a transmission of 80%. This first result gave impulse to the use of more complex integrated devices for high-field laser physics research.

A first demonstration of HHG in a complex microfluidic device was presented by Ciriolo et al. [71]. In this device a microfluidic network is used to deliver helium gas into a 6mm long cylindrical channel, which is also designed to work as a hollow optical waveguide (internal diameter 120 μm) for the driving laser (wavelength 800 nm), see Fig. 2(d). Thanks to numerical simulations (Comsol), it was demonstrated that the helium gas density inside the channel scaled linearly with the backing pressure, thus allowing to control the density of the high order harmonic generation medium. The interaction of the confined driving field with the gas molecules inside the channel resulted in HHG with a higher yield than in the more traditional generation configuration with a gas jet, as shown in Fig 2(e). This device has been further improved later on [72], increasing the length (8mm) and inner diameter (130 μm), in order to increase HHG efficiency and spectral extension. In an attempt to demonstrate the improvement due to the gas density control inside the channel a theoretical model was developed that took into account the propagation of the driving field in the gas filled hollow waveguide, showing a good agreement with the experimental results. The smoothing of the channel walls, after a thermal annealing step [73], gave a further improvement in the generation yield and a reshaping of the generated spectra in helium that is still under investigation.

Optical Materials EXPRESS

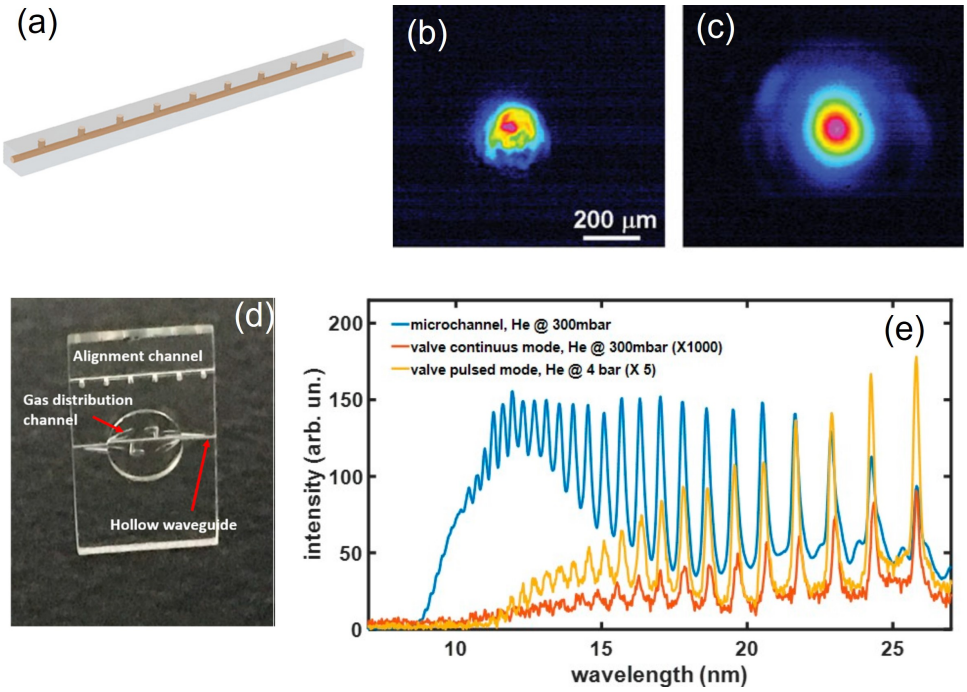

Fig. 2. (a) Schematic of the hollow waveguide fabricated by [69] , (b) Near-field and (c) far-field mode profiles of output pulses from the previous hollow waveguide with high input pulse energy of 906 μJ; (d) picture of the HHG glass chip with 6 mm length [71] and (e) comparison between HHG spectra produced inside the microchannel (blue), in a continuous gas jet (red), and in a pulsed gas jet (yellow) with He gas.

These achievements mark a substantial breakthrough in ultrafast technology, potentially making HHG-based sources available for application in numerous novel fields. Moreover we foresee that the 3D capabilities of FLICE could be further exploited for the development of more complicated integrated devices, that will be used to manipulate and control strong laser field and XUV radiation, thus paving the way for future ultrafast spectroscopy on a chip.

3.3. Astrophotonics

The field of astrophotonics promises to improve the observation of celestial objects by interfacing photonic integrated circuits with telescopes [74]. As a matter of fact, the confinement and the filtering capabilities of single-mode waveguides enable an improvement in the quality of the collected light [75], while the use of more complex integrated elements such as beam combiners and gratings provides for instance an enhancement of the angular resolution in the imaging of astronomical objects [76], or the possibility to perform the spectral analysis of the light emitted by a star [77]. In this regard, photonic integrated circuits inscribed in glass by FLM have some peculiar advantages if compared to other platforms. First, they can propagate a wide wavelength range, spanning in the visible, near and mid infrared spectra with very good performances in terms of insertion losses and reproducibility. In addition, their low birefringence is beneficial for achieving a polarization insensitive operation, a feature that allows to increase the throughput of the already faint celestial light, since no polarization filtering at their input is required. Finally, the possibility of exploiting all the three dimensions allows the inscription of complex 3D circuits capable of performing unique tasks in a reduced footprint. In the following, we will provide a brief overview about the main applications of FLM in glass for astrophotonics.

Optical Materials EXPRESS

3.3.1. Photonic lanterns and remappers

One of the first astrophotonic applications of femtosecond laser written circuits has been related to the conversion from multi-mode (MM) to single-mode (SM) operation of the celestial light. In fact, most of the instrumentation used for its processing and analysis, such as frequency filtering and phase preservation, requires a single-mode input. However, for increasing the throughput and thus collecting more photons, a multi-mode operation is preferred at the telescope output. While directly coupling a MM fiber to a SM one drops the overall light transmission, a low-loss conversion can be performed by a photonic lantern [78]. The state of the art in this respect involves fiber bundles or multicore fibers that are properly tapered to create a single multimode region at one of their ends [79]. This approach allows to convert a multimode input into hundreds of cores with an average transition loss <0.3 dB [80]. However, when stability and compactness are desired, thanks to its 3D capability, FLM is a good alternative for obtaining an integrated photonic lantern in glass. Such a device can be realized by inscribing single-mode waveguides whose cores, initially arranged very close to create a MM guiding region, are adiabatically separated in such a way to support only the fundamental mode at the end of the transition. In 2011, Thomson et al. [81] reported one of the first examples of integrated photonic lantern by employing the three-dimensional geometry presented in Fig. 3(a). The device, fabricated in borosilicate glass, was composed by 16 waveguides evolving from a MM square region of side $\sim$ 32 µm to a 4×4 square lattice of single mode waveguides spaced by 50 µm. Notably, the possibility to inscribe the waveguides without interruptions between the elements composing the device enabled a transition loss at the wavelength of 1539 nm of 0.7 dB, thus providing good performances if compared to the state of the art.

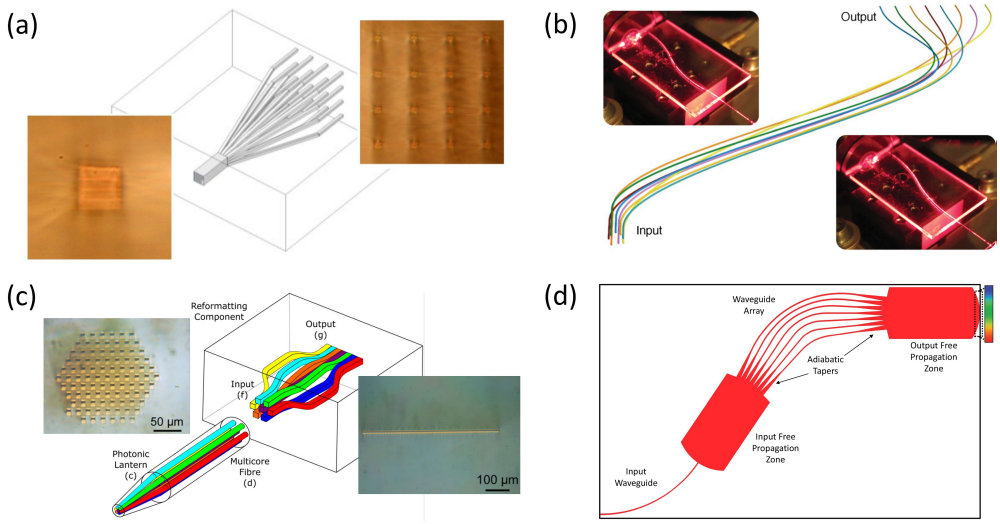

Fig. 3. a) Scheme of the photonic lantern, adiabatically converting a MM input into a 4x4 single-mode waveguide array. At the two sides, the microscope images of the input and output cross section of the device are shown. From [81]. b) Design and images of the 8 waveguides pupil remapper. The structure is bending for providing a reduction of the uncoupled light at the device output, thus increasing the signal to noise ratio. From [84]. c) Schematic and microscope images of the 92 waveguides pupil reformatter, used to convert the output of a photonic lantern into a planar waveguide. From [86]. d) Scheme of an AWG used for light dispersion. From [30].

Another field that could benefit from the 3D capability of FLM is represented by the aperture masking interferometry [82]. In this framework, the light imaged on the telescope pupil plane is

Optical Materials EXPRESS

sampled, by means of a mask or a segmented mirror, only in some points, that are then made interfere to generate a pattern containing information about the initial light distribution. This technique provides enhanced resolution and robustness to atmospheric aberrations if compared to classical imaging, and for this reason it is widely used when studying far astronomical objects [83]. Integrated optical waveguides can be used to remap the initial configuration of the sampled points into an arrangement that is more straightforward to analyze, e.g. a linear one. Moreover, the wavefront filtering provided by single-mode operation is beneficial to increase the fringe visibility. However, the three-dimensionality required to remap the sampled points from a 2D configuration to an arbitrary one cannot be achieved by planar lithographic techniques, for this reason FLM has a key role in this field. An example in this respect is represented by the pupil remapper reported in [84], shown in Fig. 3(b). The device consisted of 8 single-mode waveguides inscribed in borosilicate glass, whose design enabled the remapping of light into a linear configuration, necessary for the spectral dispersion of the resulting interference pattern. Notably, the different waveguide geometry was engineered by using 3D cubic spline interpolations to match their optical path with an error lower than 100 nm, thus enabling the temporal overlap of the remapped light. This circuit was used in an actual astronomic observation of extra-solar planets in the near infrared spectrum, performed in May 2011 at the Siding Spring Observatory, in Australia. Moreover, a recent version of it has been coupled with a planar silica-on-insulator interferometer, providing the possibility of combining up to eight telescope apertures with an overall throughput of 26% [85]. An even more complex reformatting device, still inscribed in borosilicate glass by FLM, was reported in [86]. As shown in Fig. 3(c), in this case the number of waveguides was increased to 92, with the purpose of remapping the output light of a multi-core fiber photonic lantern into a linear array of pitch equal to 6.2 μm, acting as a planar slab waveguide. Also this circuit was validated on sky, in October 2014 at the William Herschel Telescope, in the Canary islands.

3.3.2. Spectroscopy

A crucial aspect in the study of the light collected by a telescope is represented by its spectral analysis, which provides for instance information about the composition of stars and planets. In this respect, the arrayed waveguide grating (AWG), an integrated device of fundamental importance in telecommunications [87], has been proposed as dispersive element in astrophotonic applications. In this circuit, the input light is coupled into several curved single-mode waveguides with different lengths, in such a way, when the different modes are combined again in a free propagation zone, every wavelength interferes constructively at a different position of the device output, thus leading to light dispersion in the horizontal direction. Since the input of an AWG should be single-mode for a reliable operation, the first proposals interfaced photo-lithographic AWGs with femtosecond laser written photonic lanterns, which are very challenging to achieve with planar platforms due to the required three-dimensionality [77]. However, in 2018 an AWG inscribed in borosilicate glass by FLM was reported for the first time [30]. The circuit, whose schematic is shown in Fig. 3(d), was composed of 19 single-mode waveguides connecting two free propagation zones, obtained by inscribing 2300 modifications with a pitch of 0.4 μm to create two planar slab waveguides with a length equal to 7.7 mm and a width of 0.9 mm. Moreover, a tapered region was introduced at the input and output of each of the 19 waveguides for reducing the transition loss. The circuit was designed to provide spectral dispersion at a wavelength of 632.8 nm, with a FSR of 22.6 nm and a resolving power of 532, with a total footprint of 35.5 x 4.3 mm^2 and a throughput equal to 11.5% across five orders. Despite the lower performances if compared to AWGs fabricated with lithographic processes, this first demonstration showed that photonic lanterns and AWGs can be monolithically integrated in the same chip to increase both stability and coupling efficiency. In fact, the authors also reported about the inscription in

Optical Materials EXPRESS

the same sample of a 3-mode photonic lantern as input of the AWG, realized during the same fabrication run to remove any coupling loss.

3.3.3. Nulling interferometry and beam combination

Femtosecond laser micromachining in glass can be also employed to inscribe integrated interferometers with peculiar characteristics and designs, allowing to perform complex analysis of astronomical targets. The first application we consider here is related to the study of extra-solar planets. Their observation, which is of fundamental importance in astronomy, is generally made difficult by the presence of the parent star, which, being several orders of magnitude brighter, easily saturates the imaging detectors [88]. To separate the light of the planet under analysis from the light emitted by the star, an integrated nulling interferometer [89] can be used. In this device, whose schematic is shown in Fig. 4(a), the light collected by two telescopes - or by two sub-apertures of the same telescope pupil - interferes in a directional coupler. Since the star and the exoplanet have two different angular position, there exists an optical phase difference between the two spatial modes that can be exploited to completely route the starlight to one output mode, thus leaving in the other one only the planet signal, which can then be further analyzed. A laser written nuller, working at 1550 nm and based on the scheme shown in Fig. 4(a), was reported in [90] and used at the Anglo-Australian Telescope, while an even more advanced version of it, working in the NIR and involving the analysis of up to six sub-apertures, is currently used at the Subaru Telescope in the Hawaii [91]. Moreover, a 3 dB directional coupler working in the band $2.0 - 2.4$ μm has been recently realized by FLM in Infrasil silica glass [92]. Its good performance in terms of achromatic behavior, achieved by a detuning of the propagation constants, and high interferometric fringes contrast (>90%) could pave the way to the realization of nullers also in the K band, where the observation of exoplanet is facilitated by the contrast reduction between starlight and planet [93].

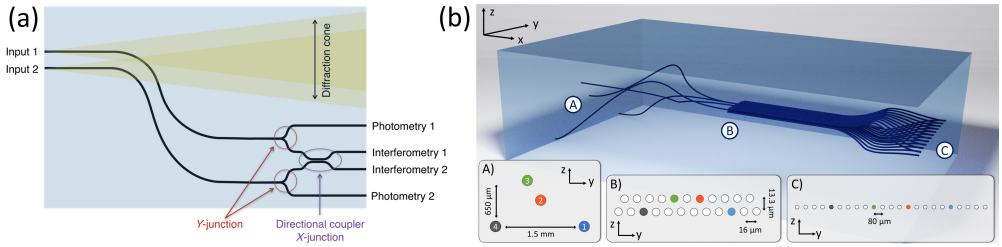

Fig. 4. a) Design of a nulling interferometer. The interference between the two spatial modes occurs in the central directional couplers, while two Y-junctions with known splitting ratio are used to estimate the input signals. The interferometer is displaced with respect to the input waveguides to reduce the disturbance of the uncoupled light. From [90]. b) Scheme of (B) the 23-modes DBC with (A) a pupil remapper and (C) a linear fan-out. From [97].

Another application worth mentioning is represented by the interferometric combination of the light beams collected by different telescopes, with the purpose of increasing the angular resolution of the observation. To perform this task, complex planar ABCD interferometers are usually used, based on the pairwise interaction of all the beams [94], a configuration which however makes it challenging to scale up the number of modes. For instance, the state-of-the-art ABCD beam combiner reported in [85] requires a total of 120 waveguides to perform the combination of 8 input modes. In this framework, a new type of device, called discrete beam combiner (DBC), has been proposed as a scalable interferometer [95]. This intrinsically 3D element is based on the continuous interference of light, achieved by means of a continuously-coupled waveguide array arranged in a triangular lattice. The continuous 3D coupling allows a reduction of the footprint of

Optical Materials EXPRESS

the device, since the beams interfere collectively and not pairwise, thus enabling a faster spreading of the input light in all the waveguides. During the astronomical observation, the properties of the target can be retrieved with an enhanced resolution from the analysis of the device output, as long as its transfer function is known. The first device based on this scheme, composed of 23 waveguides and realized in GLS for operation at 3.39 μm, showed good interference fringes contrast (87 – 93%) among the four inputs [96]. A second DBC, inscribed in borosilicate glass for guiding light at 1550 nm, was tested on sky at the William Herschel Telescope in 2019 [97]. Also in this case, the circuit (Fig. 4(b)) was a 4-input DBC with 23 waveguides, however it was followed by a fan-out region reformatting the output modes in a linear configuration. Then, the interferometer was preceded by a length-matched pupil remapper, necessary to route the four selected sub-apertures of the telescope pupil into the interferometric region. Notably, the device showed a polarization insensitive behavior, thus enabling the analysis of all the collected light without polarization filtering. Moreover, the monolithic integration of the three components in the same chip enabled an overall throughput of 50%. The DCB concept has been further scaled up in [98], where the authors realized a 6-inputs beam combiner composed of 41 waveguides and working in the J band, with central wavelength equal to 1300 nm.

4. Conclusions

Femtosecond laser micromachining has proved over the past years to be a valuable platform for the processing of glass. Thanks to the nonlinear interaction between the substrate and the ultrashort laser pulses, it is possible to inscribe 3D photonic integrated circuits with low loss, as well as to directly microstructure the substrate for the fabrication of buried microchannels and even more complex optical elements, such as lenses and filters. As we discussed, this versatility can be exploited in different fields of science and technology. In biology, femtosecond laser written microfluidic channels can provide a high control of the cells flowing in a lab-on-a-chip device, while optical waveguides and lenses allow probing their properties in an automatized way. Microchannels can also be used as hollow core waveguides to guide strong laser fields in gases for high harmonic generation. By engineering the shape of these structures, it is possible to obtain a more efficient phase matching condition if compared to bulk setups, thus providing stronger signals. Finally, we discussed the use of FLM photonic circuits in astrophotonics, where some of their main features, such as the 3D capability and the low birefringence, are exploited to the maximum for providing high-quality devices for the manipulation and analysis of the celestial light collected by telescopes.

FLM allows the integration in the same chip of several functionalities, providing complete and compact circuits. This feature evidently is important in lab-on-a-chip devices for biophotonic analysis, however, also the other applications here discussed would benefit from this integration. For instance, the fabrication of a filtering stage in the HHG generation device would allow the suppression of the remaining driving laser field in the output signal, a task currently achieved by metallic filters, which however degrade in time and are affected by a narrow bandwidth. Concerning the astronomical applications, a complete device could be for instance composed by a remapping stage, followed in the same chip by an interferometer and a spectrometer, thus gaining both interferometric and spectral information about the astronomical object under study. Moreover, the possibility to use different glasses, each of them optimized for a specific wavelength, could be exploited for analyzing the light emitted by the same target on a larger bandwidth than a single device would allow.

The versatility of FLM is also beneficial for other fields, not discussed in this review, including integrated quantum photonics, telecommunications and sensing. Moreover, the possibility to inscribe directly in the substrate integrated waveplates and polarizing beam splitters enables the on-chip manipulation of the polarization degree of freedom [99,100], a very challenging result to achieve with other platforms. Although this review is focused on glass materials, it may be

Optical Materials EXPRESS

worth mentioning that FLM can also be exploited to process crystals [101–103]. This opens up new application fields as integrated single photon sources [104] and memories [105]. The multidisciplinarity of FLM is for sure what makes it so interesting, and considering the young age of this technology, we believe that in the future the number of applications benefiting from it will further increase.

Funding. European Union through the following programs:H2020 European Research Council (742745); H2020 Future and Emerging Technologies (801336, 964588).

Disclosures. The authors declare that there are no conflicts of interest related to this article.

Data availability. No data were generated or analyzed in the presented research.

References

1. "Glass is the hidden gem in a carbon-neutral future," *Nature* **599**(7883), 7–8 (2021).
2. G. C. Righini and A. Chiappini, "Glass optical waveguides: a review of fabrication techniques," Opt. Eng. **53**(7), 071819 (2014).
3. J. Hwang, Y. H. Cho, M. S. Park, and B. H. Kim, "Microchannel fabrication on glass materials for microfluidic devices," Int. J. Precis. Eng. Manuf. **20**(3), 479–495 (2019).
4. T. Tang, Y. Yuan, Y. Yalikun, Y. Hosokawa, M. Li, and Y. Tanaka, "Glass based micro total analysis systems: Materials, fabrication methods, and applications," Sens. Actuators, B **339**, 129859 (2021).
5. R. Osellame, H. J. Hoekstra, G. Cerullo, and M. Pollnau, "Femtosecond laser microstructuring: an enabling tool for optofluidic lab-on-chips," Laser Photonics Rev. **5**(3), 442–463 (2011).
6. K. Sugioka, J. Xu, D. Wu, Y. Hanada, Z. Wang, Y. Cheng, and K. Midorikawa, "Femtosecond laser 3d micromachining: a powerful tool for the fabrication of microfluidic, optofluidic, and electrofluidic devices based on glass," Lab Chip **14**(18), 3447–3458 (2014).
7. B. N. Chichkov, C. Momma, S. Nolte, F. Von Alvensleben, and A. Tünnermann, "Femtosecond, picosecond and nanosecond laser ablation of solids," Appl. Phys. A **63**(2), 109–115 (1996).
8. R. R. Gattass and E. Mazur, "Femtosecond laser micromachining in transparent materials," Nat. Photonics **2**(4), 219–225 (2008).
9. R. Stoian and J.-P. Colombier, "Advances in ultrafast laser structuring of materials at the nanoscale," Nanophotonics **9**(16), 4665–4688 (2020).
10. F. Sima and K. Sugioka, "Ultrafast laser manufacturing of nanofluidic systems," Nanophotonics **10**(9), 2389–2406 (2021).
11. D. Tan, Z. Wang, B. Xu, and J. Qiu, "Photonic circuits written by femtosecond laser in glass: improved fabrication and recent progress in photonic devices," Adv. Photonics **3**(02), 024002 (2021).
12. X. Wang, H. Yu, P. Li, Y. Zhang, Y. Wen, Y. Qiu, Z. Liu, Y. Li, and L. Liu, "Femtosecond laser-based processing methods and their applications in optical device manufacturing: A review," Opt. Laser Technol. **135**, 106687 (2021).
13. J. He, B. Xu, X. Xu, C. Liao, and Y. Wang, "Review of femtosecond-laser-inscribed fiber bragg gratings: Fabrication technologies and sensing applications," Photonic Sens. **11**(2), 203–226 (2021).
14. G. Corrielli, A. Crespi, and R. Osellame, "Femtosecond laser micromachining for integrated quantum photonics," Nanophotonics **10**(15), 3789–3812 (2021).
15. T. T. Fernandez, S. Gross, K. Privat, B. Johnston, and M. Withford, "Designer glasses-future of photonic device platforms," Adv. Funct. Mater. **32**(3), 2103103 (2022).
16. K. Sugioka and Y. Cheng, "Femtosecond laser three-dimensional micro-and nanofabrication," Appl. Phys. Rev. **1**(4), 041303 (2014).
17. K. M. Davis, K. Miura, N. Sugimoto, and K. Hirao, "Writing waveguides in glass with a femtosecond laser," Opt. Lett. **21**(21), 1729–1731 (1996).
18. M. Will, S. Nolte, B. N. Chichkov, and A. Tünnermann, "Optical properties of waveguides fabricated in fused silica by femtosecond laser pulses," Appl. Opt. **41**(21), 4360–4364 (2002).
19. J. Hernandez-Rueda, J. Clarijs, D. van Oosten, and D. M. Krol, "The influence of femtosecond laser wavelength on waveguide fabrication inside fused silica," Appl. Phys. Lett. **110**(16), 161109 (2017).
20. T. T. Fernandez, S. Gross, A. Arriola, K. Privat, and M. J. Withford, "Revisiting ultrafast laser inscribed waveguide formation in commercial alkali-free borosilicate glasses," Opt. Express **28**(7), 10153–10164 (2020).
21. S. Piacentini, T. Vogl, G. Corrielli, P. K. Lam, and R. Osellame, "Space qualification of ultrafast laser-written integrated waveguide optics," Laser Photonics Rev. **15**(2), 2000167 (2021).
22. B. H. Babu, M. Niu, T. Billotte, P. Bi, F. Zheng, B. Poumellec, M. Lancry, and X.-T. Hao, "Femtosecond laser processing induced low loss waveguides in multicomponent glasses," Opt. Mater. Express **7**(10), 3580–3590 (2017).
23. A. Arriola, S. Gross, N. Jovanovic, N. Charles, P. G. Tuthill, S. M. Olaizola, A. Fuerbach, and M. J. Withford, "Low bend loss waveguides enable compact, efficient 3d photonic chips," Opt. Express **21**(3), 2978–2986 (2013).
24. J. W. Chan, T. Huser, S. Risbud, and D. Krol, "Structural changes in fused silica after exposure to focused femtosecond laser pulses," Opt. Lett. **26**(21), 1726–1728 (2001).
25. L. A. Fernandes, J. R. Grenier, P. R. Herman, J. S. Aitchison, and P. V. Marques, "Stress induced birefringence tuning in femtosecond laser fabricated waveguides in fused silica," Opt. Express **20**(22), 24103–24114 (2012).

Optical Materials EXPRESS

26. S. M. Eaton, H. Zhang, P. R. Herman, F. Yoshino, L. Shah, J. Bovatsek, and A. Y. Arai, "Heat accumulation effects in femtosecond laser-written waveguides with variable repetition rate," Opt. Express **13**(12), 4708–4716 (2005).
27. T. Fernandez, M. Sakakura, S. Eaton, B. Sotillo, J. Siegel, J. Solis, Y. Shimotsuma, and K. Miura, "Bespoke photonic devices using ultrafast laser driven ion migration in glasses," Prog. Mater. Sci. **94**, 68–113 (2018).
28. M. Macias-Montero, F. Mu noz, B. Sotillo, J. Del Hoyo, R. Ariza, P. Fernandez, J. Siegel, and J. Solis, "Femtosecond laser induced thermophoretic writing of waveguides in silicate glass," Sci. Rep. **11**(1), 8390 (2021).
29. G. Corrielli, S. Atzeni, S. Piacentini, I. Pitsios, A. Crespi, and R. Osellame, "Symmetric polarization-insensitive directional couplers fabricated by femtosecond laser writing," Opt. Express **26**(12), 15101–15109 (2018).
30. G. Douglass, F. Dreisow, S. Gross, and M. Withford, "Femtosecond laser written arrayed waveguide gratings with integrated photonic lanterns," Opt. Express **26**(2), 1497–1505 (2018).
31. L. B. Fletcher, J. J. Witcher, N. Troy, S. T. Reis, R. K. Brow, R. M. Vazquez, R. Osellame, and D. M. Krol, "Femtosecond laser writing of waveguides in zinc phosphate glasses," Opt. Mater. Express **1**(5), 845–855 (2011).
32. L. B. Fletcher, J. J. Witcher, N. Troy, S. T. Reis, R. K. Brow, and D. M. Krol, "Effects of rare-earth doping on femtosecond laser waveguide writing in zinc polyphosphate glass," J. Appl. Phys. **112**(2), 023109 (2012).
33. A. Abou Khalil, J.-P. Bérubé, S. Danto, J.-C. Desmoulin, T. Cardinal, Y. Petit, R. Vallée, and L. Canioni, "Direct laser writing of a new type of waveguides in silver containing glasses," Sci. Rep. **7**(1), 11124 (2017).
34. J. Hernandez-Rueda, N. W. Troy, P. Freudenberger, R. K. Brow, and D. M. Krol, "Femtosecond laser-matter interactions in ternary zinc phosphate glasses," Opt. Mater. Express **8**(12), 3622–3634 (2018).
35. A. Ródenas, G. Martin, B. Arezki, N. Psaila, G. Jose, A. Jha, L. Labadie, P. Kern, A. Kar, and R. Thomson, "Three-dimensional mid-infrared photonic circuits in chalcogenide glass," Opt. Lett. **37**(3), 392–394 (2012).
36. M. R. Vázquez, B. Sotillo, S. Rampini, V. Bharadwaj, B. Gholipour, P. Fernández, R. Ramponi, C. Soci, and S. M. Eaton, "Femtosecond laser inscription of nonlinear photonic circuits in gallium lanthanum sulphide glass," JPhys Photonics **1**(1), 015006 (2018).
37. M. D. Mackenzie, J. M. Morris, C. R. Petersen, A. Ravagli, C. Craig, D. W. Hewak, H. T. Bookey, O. Bang, and A. K. Kar, "Gls and glsse ultrafast laser inscribed waveguides for mid-ir supercontinuum generation," Opt. Mater. Express **9**(2), 643–651 (2019).
38. D. Lancaster, S. Gross, A. Fuerbach, H. E. Heidepriem, T. Monro, and M. Withford, "Versatile large-mode-area femtosecond laser-written tm: Zblan glass chip lasers," Opt. Express **20**(25), 27503–27509 (2012).
39. S. Gross, N. Jovanovic, A. Sharp, M. Ireland, J. Lawrence, and M. J. Withford, "Low loss mid-infrared zblan waveguides for future astronomical applications," Opt. Express **23**(6), 7946–7956 (2015).
40. Y. Liao, J. Qi, P. Wang, W. Chu, Z. Wang, L. Qiao, and Y. Cheng, "Transverse writing of three-dimensional tubular optical waveguides in glass with a slit-shaped femtosecond laser beam," Sci. Rep. **6**(1), 1–6 (2016).
41. S. Richter, M. Heinrich, S. Döring, A. Tünnermann, S. Nolte, and U. Peschel, "Nanogratings in fused silica: Formation, control, and applications," J. Laser Appl. **24**(4), 042008 (2012).
42. Z. Liu, J. Xu, Z. Lin, J. Qi, X. Li, A. Zhang, J. Lin, J. Chen, Z. Fang, Y. Song, W. Chu, and Y. Cheng, "Fabrication of single-mode circular optofluidic waveguides in fused silica using femtosecond laser microfabrication," Opt. Laser Technol. **141**, 107118 (2021).
43. S. Kiyama, S. Matsuo, S. Hashimoto, and Y. Morihira, "Examination of etching agent and etching mechanism on femtosecond laser microfabrication of channels inside vitreous silica substrates," J. Phys. Chem. C **113**(27), 11560–11566 (2009).
44. S. LoTurco, R. Osellame, R. Ramponi, and K. Vishnubhatla, "Hybrid chemical etching of femtosecond laser irradiated structures for engineered microfluidic devices," J. Micromech. Microeng. **23**(8), 085002 (2013).
45. E. Casamenti, S. Pollonghini, and Y. Bellouard, "Few pulses femtosecond laser exposure for high efficiency 3d glass micromachining," Opt. Express **29**(22), 35054–35066 (2021).
46. D. Bischof, M. Kahl, and M. Michler, "Laser-assisted etching of borosilicate glass in potassium hydroxide," Opt. Mater. Express **11**(4), 1185–1195 (2021).
47. A. Crespi, R. Osellame, and F. Bragheri, "Buried microchannels in alumino-borosilicate glass by femtosecond laser pulses and chemical etching," in *The European Conference on Lasers and Electro-Optics*, (Optical Society of America, 2019), p. cm_8_1.
48. M. Masuda, K. Sugioka, Y. Cheng, N. Aoki, M. Kawachi, K. Shihoyama, K. Toyoda, H. Helvajian, and K. Midorikawa, "3-d microstructuring inside photosensitive glass by femtosecond laser excitation," Appl. Phys. A **76**(5), 857–860 (2003).
49. Y. Hanada, K. Sugioka, H. Kawano, I. S. Ishikawa, A. Miyawaki, and K. Midorikawa, "Nano-aquarium for dynamic observation of living cells fabricated by femtosecond laser direct writing of photostructurable glass," Biomed. Microdevices **10**(3), 403–410 (2008).
50. Y. Hanada, K. Sugioka, H. Kawano, I. S. Ishikawa, A. Miyawaki, and K. Midorikawa, "Nano-aquarium with microfluidic structures for dynamic analysis of cryptomonas and phormidium fabricated by femtosecond laser direct writing of photostructurable glass," Appl. Surf. Sci. **255**(24), 9893–9897 (2009).
51. Y. Hanada, K. Sugioka, I. Shihira-Ishikawa, H. Kawano, A. Miyawaki, and K. Midorikawa, "3d microfluidic chips with integrated functional microelements fabricated by a femtosecond laser for studying the gliding mechanism of cyanobacteria," Lab Chip **11**(12), 2109–2115 (2011).
52. A. Schaap, Y. Bellouard, and T. Rohrlack, "Optofluidic lab-on-a-chip for rapid algae population screening," Biomed. Opt. Express **2**(3), 658–664 (2011).

Optical Materials EXPRESS

53. A. Schaap, T. Rohrlack, and Y. Bellouard, "Optical classification of algae species with a glass lab-on-a-chip," Lab Chip **12**(8), 1527–1532 (2012).
54. L. Qiao, F. He, C. Wang, Y. Cheng, K. Sugioka, and K. Midorikawa, "A microfluidic chip integrated with a microoptical lens fabricated by femtosecond laser micromachining," Appl. Phys. A **102**(1), 179–183 (2011).
55. F. He, Y. Cheng, L. Qiao, C. Wang, Z. Xu, K. Sugioka, K. Midorikawa, and J. Wu, "Two-photon fluorescence excitation with a microlens fabricated on the fused silica chip by femtosecond laser micromachining," Appl. Phys. Lett. **96**(4), 041108 (2010).
56. Y. Hu, S. Rao, and S. Wu, *et al.*, "All-glass 3d optofluidic microchip with built-in tunable microlens fabricated by femtosecond laser-assisted etching," Adv. Opt. Mater. **6**(9), 1701299 (2018).
57. P. Paiè, F. Bragheri, T. Claude, and R. Osellame, "Optofluidic light modulator integrated in lab-on-a-chip," Opt. Express **25**(7), 7313–7323 (2017).
58. J. Dudutis, J. Pipiras, S. Schwarz, S. Rung, R. Hellmann, G. Račiukaitis, and P. Gečys, "Laser-fabricated axicons challenging the conventional optics in glass processing applications," Opt. Express **28**(4), 5715–5730 (2020).
59. F. Zhang, C. Wang, K. Yin, X. Dong, Y. Song, Y. Tian, and J. Duan, "Quasi-periodic concave microlens array for liquid refractive index sensing fabricated by femtosecond laser assisted with chemical etching," Sci. Rep. **8**(1), 2419 (2018).
60. Z. Wang, K. Sugioka, and K. Midorikawa, "Three-dimensional integration of microoptical components buried inside photosensitive glass by femtosecond laser direct writing," Appl. Phys. A **89**(4), 951–955 (2007).
61. F. Sala, P. Paié, R. Martínez Vázquez, R. Osellame, and F. Bragheri, "Effects of thermal annealing on femtosecond laser micromachined glass surfaces," Micromachines **12**(2), 180 (2021).
62. P. Paiè, F. Bragheri, A. Bassi, and R. Osellame, "Selective plane illumination microscopy on a chip," Lab Chip **16**(9), 1556–1560 (2016).
63. F. Sala, M. Castriotta, P. Paiè, A. Farina, A. D'Annunzio, A. Zippo, R. Osellame, F. Bragheri, and A. Bassi, "High-throughput 3D imaging of single cells with light-sheet fluorescence microscopy on chip," Biomed. Opt. Express **11**(8), 4397–4407 (2020).
64. R. Memeo, P. Paiè, F. Sala, M. Castriotta, C. Guercio, T. Vaccari, R. Osellame, A. Bassi, and F. Bragheri, "Automatic imaging of drosophila embryos with light sheet fluorescence microscopy on chip," J. Biophotonics **14**(3), e202000396 (2021).
65. M. Lewenstein, P. Balcou, M. Y. Ivanov, A. L'huillier, and P. B. Corkum, "Theory of high-harmonic generation by low-frequency laser fields," Phys. Rev. A **49**(3), 2117–2132 (1994).
66. M. Khalil and S. Mukamel, "Ultrafast spectroscopy and diffraction from XUV to X-ray," (2020).
67. C. P. Schwartz, S. L. Raj, and S. Jamnuch, *et al.*, "Angstrom-resolved interfacial structure in buried organic-inorganic junctions," Phys. Rev. Lett. **127**(9), 096801 (2021).
68. S. Kühn, M. Dumergue, and S. Kahaly, *et al.*, "The eli-alps facility: the next generation of attosecond sources," J. Phys. B: At., Mol. Opt. Phys. **50**(13), 132002 (2017).
69. T. Popmintchev, M.-C. Chen, and D. Popmintchev, *et al.*, "Bright coherent ultrahigh harmonics in the kev x-ray regime from mid-infrared femtosecond lasers," Science **336**(6086), 1287–1291 (2012).
70. F. He, J. Lin, and Y. Cheng, "Fabrication of hollow optical waveguides in fused silica by three-dimensional femtosecond laser micromachining," Appl. Phys. B **105**(2), 379–384 (2011).
71. A. G. Ciriolo, R. M. Vázquez, A. Roversi, A. Frezzotti, C. Vozzi, R. Osellame, and S. Stagira, "Femtosecond laser-micromachining of glass micro-chip for high order harmonic generation in gases," Micromachines **11**(2), 165 (2020).
72. A. G. Ciriolo, R. M. Vázquez, and V. Tosa, *et al.*, "High-order harmonic generation in a microfluidic glass device," JPhys Photonics **2**(1), 024005 (2020).
73. R. Martínez Vázquez, A. G. Ciriolo, G. Crippa, V. Tosa, F. Sala, M. Devetta, C. Vozzi, S. Stagira, and R. Osellame, "Femtosecond laser micromachining of integrated glass devices for high-order harmonic generation," Int. J. Appl. Glass Sci. **13**(2), 162–170 (2022).
74. S. Minardi, R. Harris, and L. Labadie, "Astrophotonics: astronomy and modern optics," Astron. Astrophys. Rev. **29**(1), 6–81 (2021).
75. C. Ruilier and F. Cassaing, "Coupling of large telescopes and single-mode waveguides: application to stellar interferometry," J. Opt. Soc. Am. A **18**(1), 143–149 (2001).
76. S. Gillessen, F. Eisenhauer, and G. Perrin, *et al.*, "Gravity: a four telescope beam combiner instrument for the vlti," Proc. SPIE **7734**, 318–337 (2010).
77. J. Bland-Hawthorn, J. Lawrence, and G. Robertson, *et al.*, "Pimms: photonic integrated multimode microspectrograph," Proc. SPIE **7735**, 317–325 (2010).
78. M. Diab, A. N. Dinkelaker, J. Davenport, K. Madhav, and M. M. Roth, "Starlight coupling through atmospheric turbulence into few-mode fibres and photonic lanterns in the presence of partial adaptive optics correction," Mon. Not. R. Astron. Soc. **501**(2), 1557–1567 (2020).
79. S. G. Leon-Saval, A. Argyros, and J. Bland-Hawthorn, "Photonic lanterns," Nanophotonics **2**(5-6), 429–440 (2013).
80. D. Noordegraaf, P. M. Skovgaard, M. D. Nielsen, and J. Bland-Hawthorn, "Efficient multi-mode to single-mode coupling in a photonic lantern," Opt. Express **17**(3), 1988–1994 (2009).
81. R. R. Thomson, T. A. Birks, S. Leon-Saval, A. K. Kar, and J. Bland-Hawthorn, "Ultrafast laser inscription of an integrated photonic lantern," Opt. Express **19**(6), 5698–5705 (2011).

Optical Materials EXPRESS

82. P. Tuthill, J. Monnier, W. Danchi, E. Wishnow, and C. Haniff, "Michelson interferometry with the keck i telescope," Publ. Astron. Soc. Pac. **112**(770), 555–565 (2000).
83. A. L. Kraus, M. J. Ireland, F. Martinache, and J. P. Lloyd, "Mapping the shores of the brown dwarf desert. i. upper scorpius," Astrophys. J. **679**(1), 762–782 (2008).
84. N. Jovanovic, P. G. Tuthill, and B. Norris, *et al.*, "Starlight demonstration of the dragonfly instrument: an integrated photonic pupil-remapping interferometer for high-contrast imaging," Mon. Not. R. Astron. Soc. **427**(1), 806–815 (2012).
85. N. Cvetojevic, B. R. Norris, S. Gross, N. Jovanovic, A. Arriola, S. Lacour, T. Kotani, J. S. Lawrence, M. J. Withford, and P. Tuthill, "Building hybridized 28-baseline pupil-remapping photonic interferometers for future high-resolution imaging," Appl. Opt. **60**(19), D33–D42 (2021).
86. D. G. MacLachlan, R. J. Harris, and I. Gris-Sánchez, *et al.*, "Efficient photonic reformatting of celestial light for diffraction-limited spectroscopy," Mon. Not. R. Astron. Soc. **464**(4), 4950–4957 (2017).
87. M. K. Smit, "New focusing and dispersive planar component based on an optical phased array," Electron. Lett. **24**(7), 385–386 (1988).
88. M. Perryman, *The Exoplanet Handbook* (Cambridge University Press, 2018).
89. J. Angel and N. Woolf, "An imaging nulling interferometer to study extrasolar planets," Astrophys. J. **475**(1), 373–379 (1997).
90. T. Lagadec, B. Norris, S. Gross, A. Arriola, T. Gretzinger, N. Cvetojevic, M.-A. Martinod, N. Jovanovic, M. Withford, and P. Tuthill, "The glint south testbed for nulling interferometry with photonics: Design and on-sky results at the Anglo-Australian telescope," Publ. Astron. Soc. Aust. **38**, e036 (2021).
91. M.-A. Martinod, B. Norris, and P. Tuthill, *et al.*, "Scalable photonic-based nulling interferometry with the dispersed multi-baseline glint instrument," Nat. Commun. **12**(1), 2465 (2021).
92. A. Benoít, F. A. Pike, and T. K. Sharma, *et al.*, "Ultrafast laser inscription of asymmetric integrated waveguide 3 db couplers for astronomical k-band interferometry at the chara array," J. Opt. Soc. Am. B **38**(9), 2455–2464 (2021).
93. J.-B. Le Bouquin, J.-P. Berger, and B. Lazareff, *et al.*, "Pionier: a 4-telescope visitor instrument at VLTI," Astron. & Astrophys **535**, A67 (2011).
94. L. Labadie and O. Wallner, "Mid-infrared guided optics: a perspective for astronomical instruments," Opt. Express **17**(3), 1947–1962 (2009).
95. A. S. Nayak, T. Poletti, T. K. Sharma, K. Madhav, E. Pedretti, L. Labadie, and M. M. Roth, "Chromatic response of a four-telescope integrated-optics discrete beam combiner at the astronomical l band," Opt. Express **28**(23), 34346–34361 (2020).
96. R. Diener, J. Tepper, L. Labadie, T. Pertsch, S. Nolte, and S. Minardi, "Towards 3d-photonic, multi-telescope beam combiners for mid-infrared astrointerferometry," Opt. Express **25**(16), 19262–19274 (2017).
97. A. S. Nayak, L. Labadie, and T. K. Sharma, *et al.*, "First stellar photons for an integrated optics discrete beam combiner at the william herschel telescope," Appl. Opt. **60**(19), D129–D142 (2021).
98. E. Pedretti, S. Piacentini, G. Corrielli, R. Osellame, and S. Minardi, "A six-apertures discrete beam combiners for j-band interferometry," Proc. SPIE **10701**, 1070116 (2018).
99. G. Corrielli, A. Crespi, R. Geremia, R. Ramponi, L. Sansoni, A. Santinelli, P. Mataloni, F. Sciarrino, and R. Osellame, "Rotated waveplates in integrated waveguide optics," Nat. Commun. **5**(1), 4249 (2014).
100. R. Heilmann, M. Gräfe, S. Nolte, and A. Szameit, "Arbitrary photonic wave plate operations on chip: realizing hadamard, pauli-x and rotation gates for polarisation qubits," Sci. Rep. **4**(1), 4118 (2015).
101. F. Chen and J. V. de Aldana, "Optical waveguides in crystalline dielectric materials produced by femtosecond-laser micromachining," Laser Photonics Rev. **8**(2), 251–275 (2014).
102. B. Ali, I. V. Litvinyuk, and M. Rybachuk, "Femtosecond laser micromachining of diamond: current research status, applications and challenges," Carbon **179**, 209–226 (2021).
103. A. Ródenas, M. Gu, G. Corrielli, P. Paiè, S. John, A. K. Kar, and R. Osellame, "Three-dimensional femtosecond laser nanolithography of crystals," Nat. Photonics **13**(2), 105–109 (2019).
104. S. Atzeni, A. S. Rab, G. Corrielli, E. Polino, M. Valeri, P. Mataloni, N. Spagnolo, A. Crespi, F. Sciarrino, and R. Osellame, "Integrated sources of entangled photons at the telecom wavelength in femtosecond-laser-written circuits," Optica **5**(3), 311–314 (2018).
105. A. Seri, G. Corrielli, D. Lago-Rivera, A. Lenhard, H. de Riedmatten, R. Osellame, and M. Mazzera, "Laser-written integrated platform for quantum storage of heralded single photons," Optica **5**(8), 934–941 (2018).